Asian Journal of Civil Engineering
https://doi.org/10.1007/s42107-022-00442-y

ORIGINAL PAPER

Thermo-mechanical behavior of fire insulated fiber-reinforced polymer (FRP) strengthened reinforced concrete square column

A. Q. Sobia[1] · H. Afifudin[2] · M. S. Hamidah[3] · I. Azmi[3]

Received: 24 November 2021 / Accepted: 2 April 2022

Abstract
Fiber-reinforced polymer (FRP), a polymer matrix composite material, has been established as one of the possible techniques to strengthen concrete beams in flexure and shear. It has demonstrated good performance in retrofitting and repairing deteriorated reinforced concrete (RC) structures. However, FRP has the tendency to lose bond with the substrate due to the low glass transition (Tg) of its matrix polymer. Currently, very little information regarding to fire endurance of FRP-strengthened RC square column and the performance for insulated FRP-strengthened RC has also not been clearly addressed. This paper presents a full-scale fire resistance experiment on unstrengthened (bare) and Carbon Fiber-Reinforced Plastic (CFRP) strengthened RC with and without insulator column specimens. Ultra-high-performance fiber-reinforced cement composite (UHPFRCC) material composed of high alumina cement (HAC) and ground granulated blast slag (GGBS) in equal proportion was used to insulate the bare RC column and the column strengthened with CFRP. Two types of UHPFRCC cladding skin with one contained only polypropylene (PP) and another one with hybrid containing PP and basalt fibers were adopted. A comparison was made between the fire endurance characteristic between strengthened and unstrengthened; those with UHPFRCC insulated and those without insulator. It was found that CFRP-strengthened columns failed 15 minutes later than the unstrengthened column. In a nutshell, the developed UHPFRCC made of equal proportion of HAC, GGBS containing only 1% PP fibers improved the fire endurance of unstrengthened and CFRP-strengthened RC column significantly.

Keywords Carbon fiber-reinforced polymer (CFRP) · Ultra-high-performance fiber-reinforced cement composite (UHPFRCC) insulation · High temperature · Strengthened RC column and fire endurance

Introduction

Consolidation of research studies, in the recent decades, has postulated fiber-reinforced polymer (FRP) composite as one of the efficient strengthening/retrofitting materials for reinforced concrete (RC) structures. This is because of the fact that FRP bears lower maintenance costs, high strength-to-weight ratio, fatigue, and electrochemical corrosion resistance (Kodur et al. 2006; Arruda et al. 2016). Upgradation of building facilities is required or repair is needed due to aging of building materials, extension of their lifetime, column degradation due to lack of maintenance, the need to carry more loads than their designed values, vehicle collision, fire/explosion, and earthquake or forcible changes in the structural system such as by removal of walls/columns or removal of slab openings (Nguyen et al. 2018). However, the use of FRP poses some major concern regarding its performance in the event of fire, because both the FRP materials and the bonding adhesive are made from organic polymers (generally epoxy), which soften around their glass transition temperature (Tg) which usually ranges between 45 and 120 °C (Mouritz and Gibson, 2006). FRP has the tendency to lose bond with the substrate due to the low Tg of epoxy; the key component of FRP matrix. FRP-strengthened RC structures are susceptible to intense deterioration when exposed

✉ M. S. Hamidah
hamid929@uitm.edu.my

[1] Department of Foundation, Engineering and Physical Sciences, University of Nottingham, Nottingham, United Kingdom

[2] Center for Civil Engineering Studies, Universiti Teknologi MARA, Cawangan Pulau Pinang, Permatang Pauh Campus, Bukit Mertajam, Pulau Pinang, Malaysia

[3] School of Civil Engineering, College of Engineering, Universiti Teknologi MARA, UiTM Shah Alam, Shah Alam, Selangor, Malaysia

Published online: 04 May 2022

to elevated temperatures, particularly in the incident of fire. Bond between concrete and FRP plays a key role in transferring of loads through shear stresses developed in the polymer matrix. Mechanical property of the polymer matrix degrades with temperature that is a possible cause for the loss of contact between FRP and concrete substrate. The variation of normalized bond strength with temperature was studied by several researchers in the past (Tommaso et al. 2001; Blontrock and Vanwalleghem, 2002; Wu et al. 2004; Klamer et al. 2005; Leone et al. 2009). On the basis of available test data on bond strength, a statistical regression analysis was conducted by Ahmed (Ahmed, 2010), who proposed the relation to calculate the variation in bond strength. In fact, the most fire resistant material, concrete has found to lose strength beyond 300 °C (Klamer et al. 2005; Leone et al. 2009), so one can imagine the performance of FRP composite under fire in which the epoxy has Tg of as low as 65 °C to 150 °C (Bisby et al. 2005).

Substantial research efforts have been undertaken to evaluate the performance of Carbon Fiber-Reinforced Polymer (CFRP) at elevated temperatures. It showed that CFRP produced by pultrusion technique (P-CFRP) experienced degradation in its tensile properties after exposed to elevated temperatures up to 700 °C (Nguyen et al. 2018). It is also shown that the P-CFRP decreased 50% of its strength at 300 °C in the thermo-mechanical condition (specimens were heated to a predefined temperature and then mechanically tested until failure) and 500 °C in the residual condition (after specimens were heated to a predefined temperature and cooled to the ambient temperature, specimens were tested), while its Young Modulus decreased by 50% at 540 °C and 570 °C in two conditions, respectively (Nguyen et al. 2018). When being subjected to the thermal load, most thermosetting resins and amorphous polymer reached its T_g, causing the matrix to soften and its mechanical properties (Young's modulus, tensile strength) decreased significantly. Therefore, the contribution of the matrix to the composite tensile strength gradually becomes negligible. This contribution decreased to zero after the total decomposition of the matrix, which is characterized by a decomposition temperature, T_d (250–500 °C) (Mouritz and Gibson, 2006; Correia et al. 2010). Therefore, due to this weakness, it is necessary to safeguard the structural members that strengthened with FRP against elevated temperature in case of fire. It is well evident that passive fire protection (PFP) may be a viable option. The most suitable PFP layer is the one that is fully compatible with the concrete substrate, having premium mechanical strength to cope with the differential thermal stresses due to temperature gradients after elevated temperature exposure (Renaud et al. 2004), non-combustible, a barrier against fire spread toward adjacent buildings, and a shield to sufficiently keep the temperature of FRP and structural elements low in case of fire.

Previous research studies on FRP-strengthened columns exposed to fire have reported that the efficacy of the FRP in confining concrete is not only reliant on the stiffness of the FRP but also on the shape of the RC (Mirmiran et al. 1998; Rochette and Labossiera, 2000; Thériault and Neale, 2000; Wang and Restrepo, 2001). Although a few research studies have been conducted, on the fire behavior of FRP-strengthened concrete circular columns (Bisby et al. 2005; Bénichou et al. 2007), only limited data exist on the performance of FRP-strengthened RC square columns. In the columns with circular cross-section, FRP confinement is more effective as compared to rectangular or square cross sections. This corroborated with the lateral expansion of circular concrete under compression, i.e., homogeneously confined in a circular column, contrasting square cross-section. In the latter, most of the confinement pressure is developed at the corners from the FRP sheet, and therefore, the corners must be rounded to avoid early failure of the FRP sheet. Thériault and Neale (Thériault and Neale, 2000) explained that the FRP wraps along the flat sides of column offer insignificant resistance to the lateral expansion, consequently leading to the fractional confinement effect from the FRP wrap. Kodur et al. (Kodur et al. 2006) investigated fire endurance behavior between unstrengthened circular and one square RC columns, circular FRP-wrapped and insulated RC columns, and one square FRP-wrapped and insulated RC columns. The satisfactory fire behavior under increased service loads for both circular and square columns was observed with more significant effect for FRP-strengthened RC. It is exhibited that circular FRP-strengthened RC possessed longer fire endurance than that of square one. So far, the most used, simple and effective equations are derived from circular column which has perfect confined effect. A minimum corner radius for rectangular column is needed for installation purpose and to protect the fibers against punching from sharp corners (Kodur et al. 2006; Rochette and Labossiera, 2000). Additionally, Jau and Huang (Jau and Huang, 2008) studied on full-scale fire test on RC rectangular column 300 mm × 400 mm of size using high-strength concrete with different thickness of concrete cover. They found that concrete with thicker cover prone to fall off earlier. On the other hand, a study conducted on circular and square thermal numerical models for predicting temperatures in concrete columns with FRP-wrapped and insulated was adequately comparable against the experimental results (Cree et al. 2012). Based on Yaqub and Bailey work (Yaqub and Bailey, 2011), circular columns benefited more compared to the square cross-section column when using FRP for improving the performance of post-heated columns in terms of compressive strength and ductility. This is attributed to the fact that square cross sections contain some ineffectively confined concrete regions and intensification of stresses at their corners, while circular sections contain fully effective confined concrete regions with GFRP or CFRP jackets. Despite the advantages of circular section, RC rectangular section was

used in the present work considering using an approach proposed by Wang and Restrepo (Wang and Restrepo, 2001) and ACI 440.2R-08 (ACI 440.2R-08, 2008).

Meanwhile, Hiremath and Yaragal (Hiremath and Yaragal, 2018) investigated the performance of Reactive Powder Concrete (RPC) at elevated temperatures from 200 to 800 °C by obtaining residual mechanical properties after exposure. Li et al. (Li et al. 2020) determined the thermal properties of RPC with hybrid fiber at the temperature of 20 to 900 °C. The thermal conductivity and specific heat of RPC are lower compared to ordinary concrete (OC) and high-strength concrete (HSC), while the thermal diffusivity coefficient is lesser than HSC, however, greater than that made of OC. From earlier studies, it is proven that dense microstructure of concrete is vulnerable to explosive spalling at elevated temperatures. The main two reasons for explosive spalling for HSC when exposed to elevated temperatures are thermal stress induced by rapid temperature rise and water vapor which may cause high pore vapor pressure. To overcome spalling of concrete, addition of fiberss, especially polypropylene (PP) fibers to concrete is well known fact in the field of construction (Hiremath and Yaragal, 2018). Alternatively, Zhang et al. (Zhang et al. 2020) suggest geopolymer concrete as a substitution material to overcome spalling in concrete from elevated temperature. Lower spalling risk in geopolymer concrete under high-temperature exposure is facilitated from the highly connected pore structures. Previously, various types of high performance cementitious composites (HPCC) were explored for the protection of RC structural members against elevated temperature. It is evident from literature review that limited research has been conducted on the FRP-strengthened columns, with and without insulation, especially with square cross-section, with concrete cover of less than 50 mm, which are not actually designed to endure standard fire. The authors believe that this study dealing with the fire resistance of insulated CFRP-strengthened RC columns could be referred to validate numerical models developed by other researchers. In addition, it also found inadequate information on the influence of elevated temperature on the ultra-high-performance fiber-reinforced cementitious (UHPFRCC) containing high alumina cement (HAC), ground granulated blast furnace slag (GGBS), and/or fly ash (FA) in conjunction with hybrid fibers (basalt and PP fibers) has been reported. This could be prospective fire resisting material for the structural components.

Experimental investigation

The experimental program is divided into several phases which are preparation of materials for Ultra-High-Performance Fiber-Reinforced Cement Composite (UHPFRCC), fabrication and preparation of full-scale rectangular columns, instrumentation, wrapping the columns with CFRP, and fire test as elaborated in the following sub-sections.

Preparation of materials for UHPFRCC

High Alumina Cement (HAC), Ground Granulated Blast Furnace Slag (GGBS), Fly Ash (FA), polypropylene fibers (PP), Basalt fiber, water, and sand were used to formulate UHPFRCC. The material compositions and its quantities for both types of UHPFRCC are shown in Table 1. The percentage reflects the total binder, while for fibers, it indicates the percentage of the total volume of UHPFRCC mix. The water–binder ratio (W/B) for both mix is 0.38. The sand–binder ratios (S/B) are 0.40 and 0.45 for UHPFRCC-1 and UHPFRCC-2, respectively.

Fabrication and preparation of full-scale rectangular columns

Steel reinforcement used in the preparation of columns was main bars of 12 mm and stirrups of 10 mm diameter (Ø). Stirrups were placed at the spacing of 200 mm center-to-center. Yield strength of main bar and stirrups was 460 MPa and 280 MPa, respectively. The reinforcement cage was then placed in the plywood formwork. After fixing, the steel reinforcement cage into the formwork, grade 40 pre-mixed concrete, ordered from local supplier was poured into the formworks and the mix proportion for the grade 40 concrete is given in Table 2. Type I Portland cement and siliceous aggregates were used in preparing concrete. The demolded RC columns were cured using gunnysack in the laboratory for another 7 days. Subsequently, the column specimens were kept in the laboratory before transferring the columns to the fire-testing laboratory. The detail of unstrengthened and strengthened RC column is shown in Fig. 1.

In total, seven short RC column specimens were cast, including four unstrengthened and three CFRP-strengthened

Table 1 Material compositions and its quantities of two types of UHPFRCC skin claddings

Types of UHPFRCC	UHPFRCC-1		UHPFRCC-2	
	Composition (%)	Quantities for a single column	Composition (%)	Quantities for a single column
HAC	50	33.6 kg	50	37.9 kg
GGBS	50	33.6 kg	35	20.83 kg
FA	–	–	15	5.7 kg
PP	1	59.7 g	1	67.33 g
Basalt fiber	–	–	0.5	596.11 g
Water		25.5 kg		24.5 kg
Sand		26.9 kg		30.3 kg

Table 2 Mix proportion of grade 40 pre-mixed concrete provided by the supplier

Raw materials	Quantity (kg/m^3)
Cement	340.0
Fine aggregates	818
Coarse aggregates (20 mm)	861
Water	185.0
Retarder	0.34 Liter/m^3
Water reducing agent	0.75 Liter/m^3
Water–cement ratio	0.54
Slump	75 mm
Unit weight	2,304 kg/m^3
Air content	2%

RC column. Two of the strengthened RC columns were clad-ded with two types of UHPFRCC both made of HAC. The details of specimen series and testing parameters are given in Table 3. The size of the full-scale column specimen was 200 mm × 200 mm × 2640 mm. The first column 'C1' was tested under ambient condition to retrieve the structural properties of a typical column under compression. Both of the unstrengthened RC column specimens (C1, C2, C6, and C7) were designed according to ACI 318–08 (ACI318–08, 2008). Column C3, C4, and C5 were strengthened with CFRP designed according to ACI 440.2R-08 (ACI 440.2R-08, 2008).

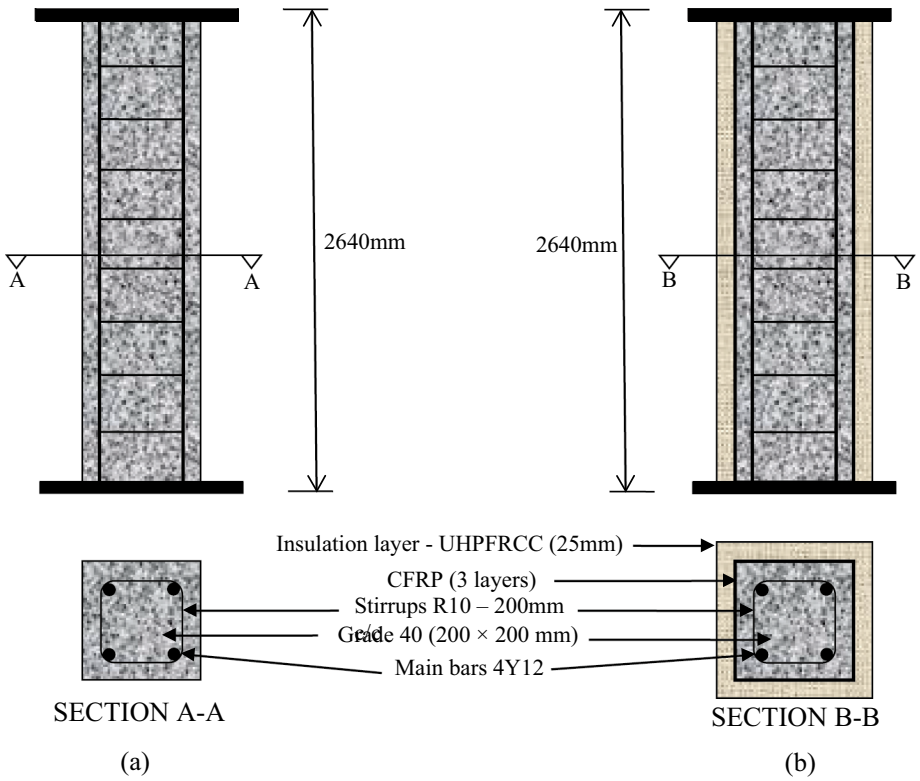

Fig. 1 **a** Unstrengthened and **b** strengthened RC column details

Table 3 Series of column specimens prepared along with testing parameters

Specimen	Type of loading	Total sustained load (KN)	Type of skin cladding
C1	Conventional loading at Ambient Temperature	–	–
C2	40% of P_u + ASTM E119 fire	468	–
C3	40% of P_u + ASTM E119 fire	574	CFRP
C4	40% of P_u + ASTM E119 fire	574	CFRP + UHPFRCC-1
C5	40% of P_u + ASTM E119 fire	574	CFRP + UHPFRCC-2
C6	40% of P_u + ASTM E119 fire	468	UHPFRCC-1
C7	40% of P_u + ASTM E119 fire	468	UHPFRCC-2

Instrumentation

After preparation of steel reinforcement cage and formwork, thermocouples were installed. Column C1 was tested at ambient temperature; the axial and the lateral deformation of the specimens were recorded using deflectometer dial gages placed at the mid span of the column. In other RC columns, prepared for fire test, thermocouples were fixed to the column specimens, to the steel bar and the location of the thermocouples are shown in Fig. 2. Thermocouples of type 'K' were installed at locations T1, T2, T3, T4, T5, T6, T7, T8, and T9. These locations include concrete core (at the depth of 100 mm), concrete surface, steel bars, and CFRP/concrete interface, to record the temperature readings from those points. The nine thermocouples were positioned at same height which is 1.3 m from the base. Except T1, for each point in column, two opposite readings were recorded, and then, their average was reported in the results.

UHPFRCC cladding over RC columns

In the end, designated Columns C4, C5, C6, and C7 were cladded with two different types of UHPFRCC namely designated as UHPFRCC-1 and UHPFRCC-2. Fresh mixture of UHPFRCC was then plastered over each of the above-mentioned columns by maintaining the thickness of 25 mm. The cladding was plastered in two layers to avoid the dropping of the plaster. After UHPFRCC cladding, the columns were remained in the laboratory and cured using tap water till the test date. UHPFRCC cladding was provided in order to protect the columns against fire and make them sustain for longer period of time.

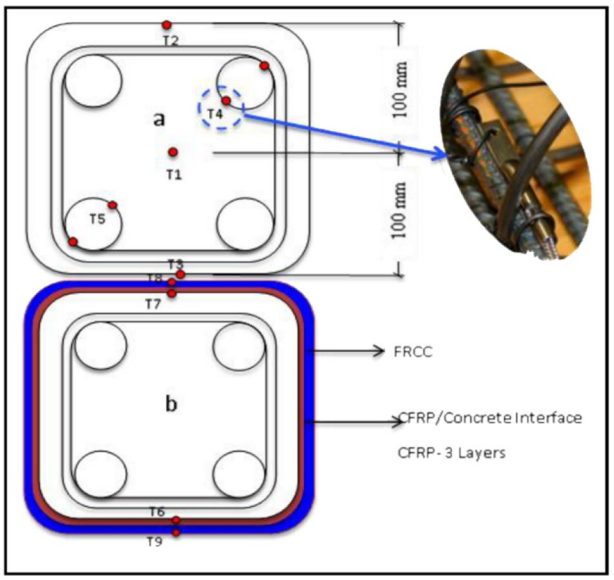

Fig. 2 The locations of thermocouples in concrete, rebar, CFRP/concrete interface, and UHPFRCC

Carbon fiber-reinforced polymer (CFRP) wrapping over RC column

After casting and curing of concrete columns, a high-strength carbon fabric; Build Seal CFFS Extra was used for strengthening of designated RC column specimens. The carbon fiber is a fabric sheet of longitudinal oriented, continuous carbon fiber filaments. The carbon fiber fabric sheet was wrapped on the designated columns. To bond between carbon fiber fabric sheet and concrete column; epoxy paste, Epo Bond CF was used. Properties of carbon fiber and epoxy are given by the manufacturers and listed in Tables 4 and 5, respectively. The mixture of epoxy and hardener was roller-applied to the wrapped carbon fiber fabric sheet on the RC column surface. The volume of epoxy is two times of the hardener.

Full-scale fire testing

In the present research, ASTM E119-15 (ASTM E119–15, 2015) fire curve was used for full-scale fire testing. Numerous equations approximating the ASTM E119 curve were reported by Lie and Woollerton (Lie and Woollerton, 1988), but the modest of all provides the temperature T (°C) as in Eq. (1)

Table 4 Properties of fibers used for strengthening of test RC columns

Property	Test value
Fiber type	Ultra-high-strength carbon
Fiber tensile strength	4900 MPa
Fiber tensile modulus	230 GPa
Thickness	0.117
Area weight	200–600 g/m^3
Style	Woven uni directional

Table 5 Properties of epoxy used in CFRP strengthening

Product name	Epo bond CF
Glass transition temperature (T_g)	82 °C
Tensile strength	72.4 MPa
Tensile modulus	3.18 GPa
Elongation percent	5.0%
Flexural strength	123.4 MPa
Flexural modulus	3.12 GPa

$$T = 750\left[1 - e^{(-3.79553\sqrt{t_b})}\right] + 170.41\sqrt{t_b} + T_0 \quad (1)$$

where t_b is time (hours) and T_0 is initial temperature.

To test RC column specimens under ASTM E119 with sustained axial concentric load, full-scale column furnace at Fire Testing Laboratory, Universiti Teknologi Malaysia (UTM), Skudai, Johor, Malaysia was used. The furnace was operated with the gas. The capacity of the loading frame was around one ton. Therefore, the length of the columns were designed short (2640 mm) to reach the plunger height, so a high-strength (Grade 60) cylindrical base lined with a circular thick plate of length 2120 mm was provided at the bottom. Steel plates were fixed on both sides of columns. The extruded main bars from the columns were first welded with the steel plate and then bolted with the base. The base was bolted with the ground to provide fix connection at the bottom. Also, the top steel plate was bolted with the test frame loading head to provide a fix connection at the top as well. The top and bottom plates as well as the plunger were protected with rock wood boards. The base was also further protected with ceramic fibers. The thermocouples were connected to the data logger and the temperature readings throughout the test were recorded. Figure 3 shows the furnace and the set up in fire-testing chamber.

Fig. 3 Full-scale furnace in fire testing laboratory at Universiti Teknologi Malaysia (UTM)

Experimental results and discussion

Column 'C1' was tested in the laboratory under room temperature to obtain the typical ambient structural properties of RC column. Column C1 experienced 1170 kN failure load and 3.05 mm maximum displacement. Columns C2, C3, C4, C5, C6 and C7 were tested under design fire exposure till they reach failure. Failure point was determined when columns were not able to sustain the applied load. The load was applied till the desired value and then was kept sustained throughout the fire test. The columns experienced an initial load, equivalent to 40% of ultimate load (P_u), from the weight of the hydraulic jack prior to the start of the preload phase, as shown in Fig. 4. Axial deformations during pre-load and fire test phase were also recorded from the instrument from the start of the experiment till the failure point, as graphically shown in Fig. 5. The witnessed axial deformations of the columns were the result of a combination of load effects and thermal expansion. It was observed that in Column C2 (unstrengthened), the axial deformations are greater than in C3 (CFRP-strengthened). In the

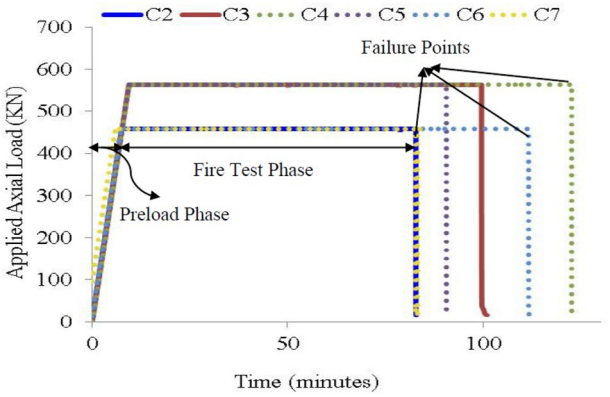

Fig. 4 Applied axial load as a function of time for all RC columns

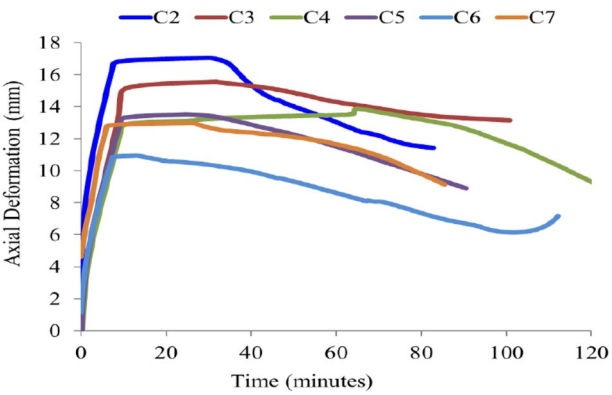

Fig. 5 Axial deformation as a function of time for all RC columns

pre-load phase, deformations linearly increased up to around 17 mm. After the start of fire test, the column expanded, for some time deformations remained constant followed by the considerable decrease, up to 12 mm at failure point, due to the contraction of column, as also reported by Kodur et al. (Kodur et al. 2005). The contraction of the column is corroborated mainly with loss of strength, stiffness of the concrete, and steel as the internal temperatures increased. Among all columns, C4 (CFRP + UHPFRCC-1) underwent the lowest contractions, which could be due to two reasons: (1) confinement effect of CFRP and (2) lower temperature within column due to the UHPFRCC-1 cladding.

Table 6 tabulates the fire resistance of all the columns exposed to ASTM E119 standard fire. It could be seen that the highest fire resistance has been marked by Column C4 that is 113 min (min), which means that the C4 failed after 113 min (~ 2 h) of fire. On contrary, the control column failed only after 75 min of fire, which is 38 min less than C4. Overall, CFRP-strengthened Columns (C4 and C5) survived the fire longer than the unstrengthened columns. Columns C6 and C7 also shows the effectiveness of CFRP along with the UHPFRCC cladding. On the other hand, as compared to UHPFRCC-1 and UHPFRCC-2, the columns cladded with UHPFRCC-1 (C4 and C6) the one that containing only PP fibers persisted longer in the fire as compared to the columns cladded with UHPFRCC-2 (C5 and C7) that made of hybrid fibers PP and basalt. It may be due to congestion of fibers, which blocked the moisture-release path created by PP fibers resulting in a thermal cracking due to pore pressure development. The lowest values marked by the column cladded with UHPFRCC-2 contained basal fibers might be due to the fact that T_g of basalt fibers was reached around 673 °C. In the same table, the failure mode for each column is also stated. Overall, almost all of the columns failed with a blasting noise.

It seems that the temperature penetrated faster in the upper one-third portion of the column. The lose portion of concrete just before the failure due to explosive spalling, resulted in the softening of rebar, leading to the failure of the control Column C2, generally, failed by the yielding of steel bar. Failure pattern of Column C2 is shown in Fig. 6(a), while failure patterns for Column C3 are shown in Fig. 6(b). The CFRP sheets remained in one piece after failure of the column and CFRP also withered partially due to the confinement effect. The excessive cracking on the surface of the column was also observed. The CFRP-strengthened RC column cladded with UHPFRCC-1, Column C4, shows that the UHPFRCC-1 has detached after fire test and the color of the cladding changed from grayish brown to pinkish brown. On contrary, failure in Column C5 was different from Column C4 even though after cladded with UHPFRCC-2. Although the cladding collapsed later than the cladding over C4 but from the failure pattern of column, it could be implied that the coating rendered ineffective quite early. Due to the early uselessness of UHPFRCC-2 cladding, the temperature inside the concrete substrate as well as rebars increased very fast resulting in the early failure. It could be observed that from more than one-third of the lower portion of column, concrete cover has been removed by exposing the steel rebar. The failure patterns of Column C4 and C5 are shown in Fig. 6(c and d), respectively. The unstrengthened RC column cladded with UHPFRCC-1, Column C6 failed in the same fashion as Column C2. The UHPFRCC-1 cladding remained partially intact after the fire test but turned to beige color (buff), indicating that the temperature in the cladding reached beyond 900 °C. While the unstrengthened RC column cladded with UHPFRCC-2, Column C7 failed in quite a different manner as compared to all other columns. Concrete cover was fully removed by exposing the rebar along with the core of concrete; however, the failure of rebar occurred at the same

Table 6 Fire resistance of columns after exposure to ASTM E119 standard fire

Column no	Types of skin cladding	Fire resistance (min)	% Ratio and increase in fire resistance (min) w.r.t control specimen	Failure mode
C2	–	75	–	Sudden and explosive failure removing concrete cover and exposing steel
C3	CFRP	90	1.20 (15 min more)	Sudden and explosive failure removing concrete cover and exposing steel
C4	CFRP + UHPFRCC-1	113	1.50 (38 min more)	Buckling of main reinforcement removing concrete cover and UHPFRCC-1
C5	CFRP + UHPFRCC-2	81	1.08 (6 min more)	Explosive spalling of concrete followed by removal of UHPFRCC-2
C6	UHPFRCC-1	102	1.36 (27 min more)	Buckling of main reinforcement removing concrete cover and UHPFRCC-1
C7	UHPFRCC-2	76	1.01 (1 min more)	Explosive spalling of concrete cover removing UHPFRCC-2 and exposing main reinforcement throughout the length of column

Fig. 6 Column **a** C2 and **b** C3 specimens before and the failure mode after exposing ASTM E119 fire test. Column **c** C4 and **d** C5 specimens before and the failure mode after exposing ASTM E119 fire test (continued). Column **e** C6 and **f** C7 specimens before and the failure mode after exposing ASTM E119 fire test (continued)

point as in column C2 and C6 which is on the upper one-third portion of the column. The failure patterns of Columns C6 and C7 are shown in Fig. 6(e and f), respectively.

Figure 7a and b show the increase in temperature as a function of time on the concrete surface and the core (at the depth of 100 mm) of concrete, respectively. While Fig. 7c shows the temperature changes in steel reinforcement during fire test. It could be noticed that the highest temperature rise occurred in the column without CFRP strengthening and UHPFRCC cladding (Column C2), which was obvious,

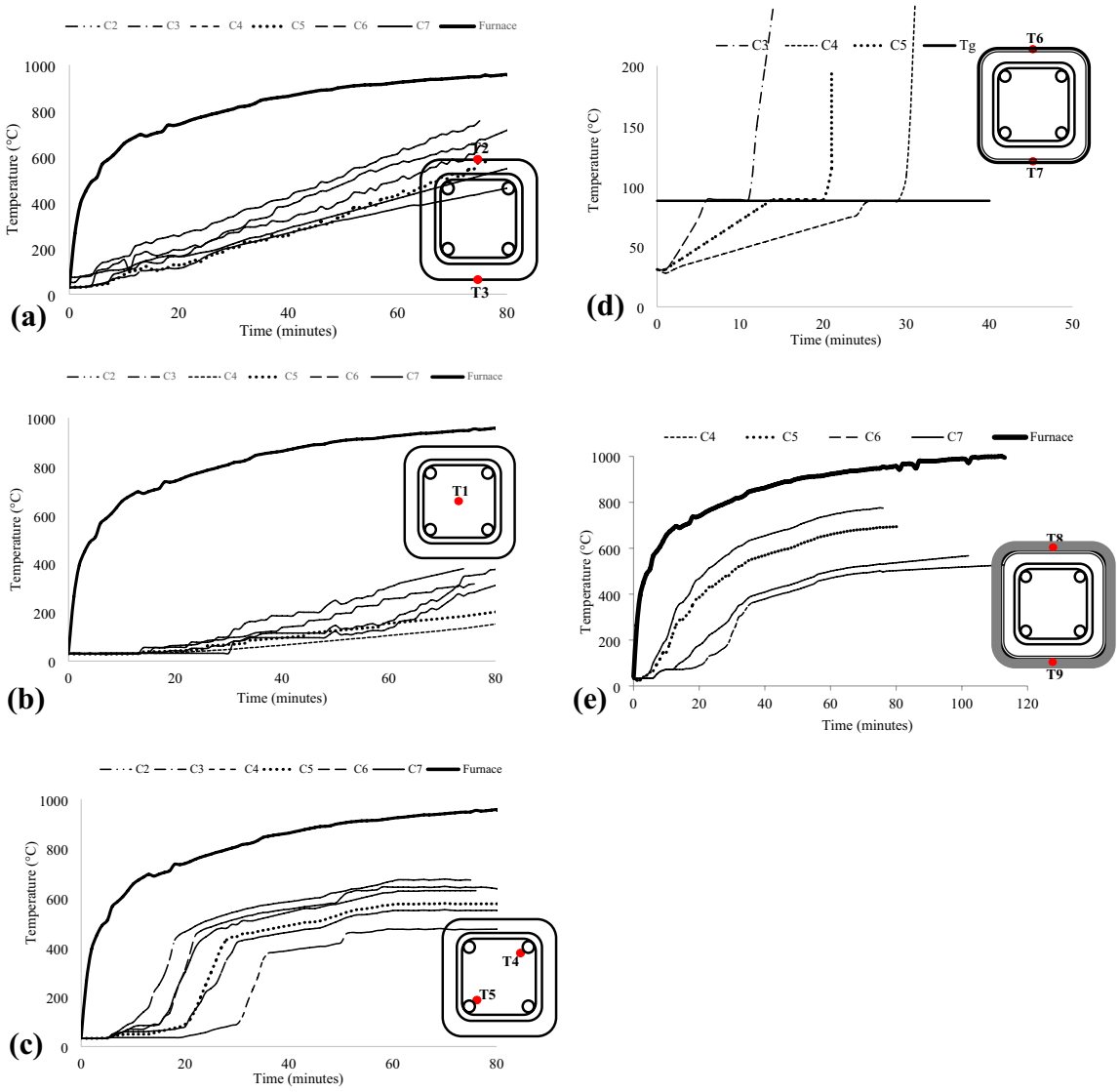

Fig. 7 **a** Concrete temperatures measured at the concrete surface of the seven RC column specimens. **b** Concrete temperatures measured at the core (the depth of 100 mm). **c** Temperature of steel reinforcement embedded in all columns. **d** Measured temperature at the CFRP concrete interface. **e** Measured temperature in UHPFRCC-1 and UH PFRCC-2 with function of time

resulting in the increased temperature in steel rebar. However, with the CFRP strengthening (Column C3) comparatively reduced temperature levels were observed both on the surface as well as in the core of concrete column. This could be corroborated with the effectiveness of CFRP fibers, which even after losing contact with concrete, due to the melting of epoxy, protected the concrete column somehow against fire. Overall, it was found that between the two types of UHPFRCC claddings, UHPFRCC-1 rendered as the most effective by the end of fire test. It could also be observed in Fig. 7a and b, where the UHPFRCC-1 cladded CFRP-strengthened RC column (Column C4) and unstrengthened RC column (Column C6) depicted reduced temperature levels as compared to the UHPFRCC-2 cladded CFRP-strengthened RC column (Column C5) and unstrengthened RC column (Column C7). This was followed by the respective increase in the steel rebar. According to Schneider (Schneider, 1988), concrete starts to lose its original compressive strength at temperature level above 200 °C. In Column C4, only after 29 min temperature surpassed 200 °C, on the surface of concrete, as compared to the control column C2, in which temperature level exceeded 200 °C after 12 min of exposure to fire. Although after 29 min, the steel rebar reached 341 °C and 541 °C in Column C4 and Column C2, respectively. Therefore, in control column, steel started to lose its yield strength quite earlier than Column C4, as in reinforcing steel, at temperature levels near 300 °C, there is a 20% drop in the initial room temperature yield strength (Lie and

Woollerton, 1988). This proves the effectiveness of UHP-FRCC-1 in protecting RC columns against fire leading to the improved fire resistance. On the other hand, in UHP-FRCC-2 cladded column, the temperature level at concrete level exceeded 200 °C, also after 29 min, however, afterward the temperature increased drastically due to which the failure time of column was reduced in comparison with C4.

For the columns strengthened with CFRP (Column C3, Column C4, and Column C5), it could predictably be stated that the FRP wraps were structurally ineffective by the termination of the fire tests, because the temperature in FRP surpassed the glass transition temperature (T_g) of the epoxy adhesive/resin (82 °C) relatively early in the fire exposure, as clearly evident from Fig. 7d. The epoxy resin has transformed from solid phase to softening phase after surpassing the Tg, losing its binding capacity in line with Wu et al. (Wu et al. 2004).

However, even though the FRP strengthening system was assumed to have been ineffective by the termination of the fire tests, the failure durations of the CFRP-strengthened RC columns (Column C3, Column C4, and Column C5) and unstrengthened RC columns (Column C2, Column C6, and Column C7) were considerably different. This might be due to the confinement effect of CFRP, in which fibers have the ability to bear high temperature as compared to the epoxy resin that has low Tg. Those carbon fibers helped to keep the temperature low initially, which extended the duration of failure as compared to the unstrengthened columns. Among all columns, as shown in Fig. 7d, in Column C4, Tg of epoxy reached in about 30 min of start of the fire test that is 20 min more than the control column. This means that UHPFRCC-1 protected the epoxy of CFRP below Tg for 20 min more than the unprotected CFRP-strengthened column and kept it bonded to the surface of concrete by keeping it effective for the longer time. Column C4 was protected by UHPFRCC-1 skin cladding, which rendered more effective as compared to UHPFRCC-2 (cladded over Column C5) when exposed to fire. In contrast, the Tg in unprotected Column C3 reached only after 10 min of fire test.

Figure 7e shows the increase in temperature in UHP-FRCC cladding as a function of time. It could be noticed that columns cladded with UHPFRCC-1 (Column C4 and Column C6) depicted the lowest increase in temperature levels during fire test. In CFRP-strengthened RC columns (Column C4 and Column C5), temperature rose beyond 200 °C after 30 min and 12 min, respectively. However, in columns without CFRP strengthening (Column C6 and Column C7), during fire test, temperature level reached beyond 200 °C after about 22 min and 10 min, respectively. Overall, this shows that CFRP-strengthened columns indicated better performance as compared to unstrengthened columns, corroborated with the contribution of CFRP fibers to protect column in conjunction with UHPFRCC-1.

Conclusions

Based on the full-scale fire experiments and analysis of the results, which were presented in this paper, the following conclusions are drawn in terms of fire resistance of RC columns:

The fire resistance of RC column strengthened with CFP was 15 min more than the unstrengthened RC column which the latter recorded reduced temperature levels both on the surface and in the core of the column.

It was concluded that CFRP reinforced RC column cladded with UHPFRCC endured fire for the longer time as compared to other columns. Protection of plain RC column with UHPFRCC containing only PP fibers increased the fire resistance of strengthened RC by 27 min as compared to the control one.

Overall, UHPFRCC (containing only PP fibers) cladding rendered more effective as compared to the UHP-FRCC cladding containing hybrid fibers. However, the former was not able to maintain the temperature of CFRP strengthening system below its T_g for the entire duration of time.

In a nutshell, the developed UHPFRCC cladding made of HAC, GGBS, and containing only 1% PP fibers improved the fire endurance of unstrengthened and CFRP-strengthened RC column significantly. In addition, the time to reach the T_g of CFRP matrix was also improved by the application of UHPFRCC skin cladding that kept the CFRP effective for longer period of time as compared to the unprotected CFRP-strengthened RC column.

Acknowledgements The authors wish to thank Universiti Teknologi MARA (UiTM), Universiti Teknologi Malaysia (UTM), and NED University of Engineering & Technology (NEDUET) for offering all the research facilities needed for conducting this research study. Especially, the authors would also like to acknowledge faculty for the future program, Ministry of Higher Education Malaysia, 600-RMI/DANA5/3 CIFI (26/2013) and Ministry of Science, Technology and Innovation (MOSTI), eScience grant No. 06-01-01-SF 0812, to provide necessary financial support to conduct this research.

Funding The authors received no financial support for the research authorship and/or publication of this article.

Declarations

Conflict of interest On behalf of all the authors, the corresponding author states that there is no conflict of interest.

References

American Concrete Institute (ACI) 440.2R-08. (2008) Guide for the design and construction of externally bonded FRP systems for

strengthening concrete structures. ACI Committee 440, American Concrete Institute. Farmington Mills, MI p. 76.

American Concrete Institute (ACI) 318–08. (2008) Building code requirements for structural concrete and commentary. American Concrete Institute. Farmington Mills, MI

Ahmed, A. (2010). *Behavior of FRP-strengthened reinforced concrete beams under fire conditions*. Michigan State University.

Arruda, M. R. T., Firmo, J. P., Correia, J. R., & Tiago, C. (2016). Numerical modelling of the bond between concrete and CFRP laminates at elevated temperatures. *Eng Struct, 110*, 233–243.

American Standard Testing and Method (ASTM) E119–15. (2015) Standard test methods for fire tests of building construction and materials. ASTM International, West Conshohocken, PA. www.astm.org

Bénichou N., Kodur, V. K. R., Chowdhury, E. U., Bisby, L. A., and Green, M. F. (2007) *Results of fire resistance experiments on FRP-strengthened reinforced concrete slabs and beam-slab assemblies– report No. 2*, National research council, Institute for Research in Construction, Research Report 234.

Bisby, L. A., Kodur, V. R., & Green, M. F. (2005). Fire endurance of fiber-reinforced polymer-confined concrete columns. *Struct J, 102*(6), 883–891.

Blontrock, H. L. T., and Vanwalleghem, H. (2002) Bond Testing of Externally Glued FRP Laminates at Elevated Temperatures, in Proceeding of the International Conference Bond in Concrete—from Research to Standards, pp. 648–654.

Correia, J. R., Branco, F. A., Ferreira, J. G., Bai, Y., & Keller, T. (2010). Fire protection systems for building floors made of pultruded GFRP profiles: Part 1: Experimental investigations. *Compos Part B Eng, 41*, 67–629.

Cree, D., Chowdhury, E. U., Green, M. F., Bisby, L. A., & Bénichou, N. (2012). Performance in fire of FRP-strengthened and insulated reinforced concrete columns. *Fire Saf J, 54*, 86–95.

Di Tommaso, A., Neubauer, U., Pantuso, A., & Rostasy, F. S. (2001). Behaviour of adhesively bonded concrete-CFRP joints at low and high temperatures. *Mech Compos Mater, 37*(4), 327–338.

Hiremath, P. N., & Yaragal, S. C. (2018). Performance evaluation of reactive powder concrete with polypropylene fibres at elevated temperatures. *Constr Build Mater, 169*, 499–512.

Jau, W. C., & Huang, K. L. (2008). A study of reinforced concrete corner columns after fire. *Cem Concr Compos, 30*, 622–638.

Klamer, E. L., Hordijk, D. A., and Janssen, H. J. M. (2005) The influence of temperature on the debonding of externally bonded CFRP," In Proceedings 7th Int. Symposium on Fiber Reinforcement Polymer Reinforcement for Concrete Structures (FRPRCS-7), pp 1551–1570.

Kodur, V. R. K., Bisby, L. A., Green, M. F., & Chowdhury, E. (2005). Fire endurance experiments on FRP-strengthened reinforced concrete columns. *National Research Council of Canada, Institute for Research in Construction, Research Report*, *185*.

Kodur, V. K. R., Bisby, L. A., & Green, M. F. (2006). Experimental evaluation of the fire behaviour of insulated fiber-reinforced-polymer-strengthened reinforced concrete columns. *Fire Saf J, 41*(7), 547–557.

Leone, M., Matthys, S., & Aiello, M. A. (2009). Effect of elevated service temperature on bond between FRP EBR systems and concrete. *Compos Part B Eng, 40*(1), 85–93.

Li, H., Hao, X., Qiao, Q., Zhang, B., & Li, H. (2020). Thermal properties of hybrid fiber-reinforced reactive powder concrete at high temperature. *J Mater Civil Eng, 32*(3), 04020022.

Lie, T. T., & Woollerton, J. L. (1988). Fire resistance of reinforced concrete columns: Test results.

Mirmiran, A., Shahawy, M., Samaan, M., Echary, H. E., Mastrapa, J. C., & Pico, O. (1998). Effects of column parameters on FRP-confined concrete. *J Compos Constr, 2*(4), 175–185.

Mouritz, A. P., & Gibson, A. G. (2006). *Fire properties of polymer composite materials*. Dordrecht: Springer.

Nguyen, P. L., Xuan, H. V., & Emmanuel, F. (2018). Elevated temperature behavior of carbon fiber-reinforced polymer applied by handlay-up (M-CFRP) under simultaneous thermal and mechanical loadings: Experimental and analytical investigation. *Fire Saf J, 100*, 103–117.

Renaud, C., Aribert, J. M., & Zhao, B. (2004) Effect of differential thermal stresses on the fire resistance of composite columns with hollow section. Fifth International Conference on Composite Construction in Steel and Concrete Kruger National Park Berg-en-Dal, Mpumalanga, South Africa, pp. 607–618.

Rochette, P., & Labossiera, P. (2000). Axial testing of rectangular column models confined with composites. *J Compo Constr, 4*(3), 129–136.

Schneider, U. (1988). Concrete at high temperatures—a general review. *Fire Saf J, 13*, 55–68.

Thériault, M., & Neale, K. W. (2000). Design equations for axially loaded reinforced concrete columns strengthened with fiber-reinforced polymer wraps. *Can J Civil Eng, 27*(5), 1011–1020.

Wang, N., Hou, S., & Jin, H. Y. (2012). Crystallization behavior of heat-treated basalt fiber. *Adv Mater Res, 560*, 3–7.

Wang, Y. C., & Restrepo, J. I. (2001). Investigation of concentrically loaded reinforced concrete columns confined with glass fiber-reinforced polymer jackets. *Struct J, 98*(3), 377–385.

Wu, Z. S., Iwashita, K., Yagashiro, S., Ishikawa, T., & Hamaguchi, Y. (2005). Temperature effect on bonding and debonding behavior between FRP sheets and concrete. *J Soc Mater Sci, 54*(5), 474–480.

Yaqub, M., & Bailey, C. G. (2011). Cross sectional shape effects on the performance of post-heated reinforced concrete columns wrapped with FRP composites. *Composite Structure, 93(3)*, 1103–1117.

Zhang, H. Y., Qiu, G. H., Kodur, V., & Yuan, Z. S. (2020). Spalling behavior of metakaolin-fly ash based geopolymer concrete under elevated temperature exposure. *Cem Concr Compos, 106*, 103483.